

Magnetic dipole transitions in the hydrogen molecule

Krzysztof Pachucki^{1,*} and Jacek Komasa^{2,†}

¹*Institute of Theoretical Physics, University of Warsaw, Hoża 69, 00-681 Warsaw, Poland*

²*Faculty of Chemistry, A. Mickiewicz University,
Grunwaldzka 6, 60-780 Poznań, Poland*

(Dated: January 25, 2011)

Abstract

In homonuclear molecules, such as H₂, the electric dipole transitions are strongly forbidden, and the transitions between rovibrational states are of the electric quadrupole type. We show however, that magnetic dipole transitions also take place, although are significantly weaker. We evaluate the probabilities of such transitions between several lowest rotational states and compare them with those of the corresponding electric quadrupole transitions.

PACS numbers: 33.15.Kr, 31.15.vn, 95.30.Ky, 33.20.Ea

*Electronic address: krp@fuw.edu.pl

†Electronic address: komasa@man.poznan.pl

I. INTRODUCTION

The rotating hydrogen molecule although neutral, has a nonvanishing magnetic moment $\vec{\mu}$, that comes from the nuclear and the electronic rotational angular momentum. For a molecule in the Σ electronic state, the expectation value of the electronic angular momentum vanishes and the electronic magnetic moment comes from the nonadiabatic effect [1, 2], the coupling of the electron to the nuclear motion. In the approximate but still quite accurate treatment, one can associate a value of the rotational magnetic moment with each distance R between the protons. The average in a rovibrational state gives the total rotational magnetic moment. The appropriate formula has been first derived by Wick [3, 4], and confirmed experimentally by Ramsey *et al.* [5–9].

Since the matrix elements of the R -dependent rotational magnetic moment between different vibrational states do not vanish, the magnetic dipole transitions are allowed, although only between states of the same rotational quantum number J . $\Delta J = 1$ transitions are strictly forbidden due to parity. The magnetic dipole transitions occur at the same wavelength as the electric quadrupole ones, thus their existence for the unpolarized sample of H_2 molecules, can be observed by the increased total transition intensities. Since the final quantum states corresponding to E2 and M1 transitions are orthogonal to each other, namely the photon states have different angular momentum, the total rate is a sum of the individual M1 and E2 rates.

In this work we employ the known formulae for the magnetic dipole moment to perform numerical calculations and verify them with the experimental values of Ramsey *et al.* [5–9]. Having checked correctness of the magnetic dipole moment as a function of the internuclear distance we perform numerical calculations of the magnetic dipole transition rates, which is our main goal. For low values of J these rates happen to be much smaller in comparison to the electric quadrupole ones, but increase quickly with J to become dominant for highly excited rotational states.

II. THE ADIABATIC APPROXIMATION

The total wave function ϕ is the solution of the stationary Schrödinger equation

$$[H - E] |\phi\rangle = 0, \quad (1)$$

with the Hamiltonian

$$H = H_{\text{el}} + H_{\text{n}}, \quad (2)$$

split into the electronic and nuclear parts. In the electronic Hamiltonian H_{el}

$$H_{\text{el}} = - \sum_a \frac{\nabla_a^2}{2 m_e} + V \quad (3)$$

the potential V includes all the Coulomb interactions with fixed positions \vec{R}_X of nuclei. The nuclear Hamiltonian involves kinetic energies of the nuclei

$$H_{\text{n}} = - \sum_{X=A,B} \frac{\nabla_{\vec{R}_X}^2}{2 M_X}. \quad (4)$$

For a diatomic molecule in the space-fixed reference frame attached to the geometrical center of the two nuclei, H_{n} takes the form

$$H_{\text{n}} = - \frac{\nabla_{\vec{R}}^2}{2 m_{\text{n}}} - \frac{\nabla_{\text{el}}^2}{2 m_{\text{n}}} - \left(\frac{1}{M_B} - \frac{1}{M_A} \right) \vec{\nabla}_{\vec{R}} \cdot \vec{\nabla}_{\text{el}}, \quad (5)$$

where $\vec{R} = \vec{R}_A - \vec{R}_B$, $\vec{\nabla}_{\text{el}} = 1/2 \sum_a \vec{\nabla}_a$, and $1/m_{\text{n}} = 1/M_A + 1/M_B$ is the nuclear reduced mass.

In the adiabatic approximation the total wave function ϕ_{a} is a product of the electronic and the nuclear wave functions

$$\phi_{\text{a}}(\vec{r}, \vec{R}) = \phi_{\text{el}}(\vec{r}) \chi(\vec{R}), \quad (6)$$

the former obeying the clamped nuclei electronic Schrödinger equation,

$$H_{\text{el}} \phi_{\text{el}} = \mathcal{E}_{\text{el}}(\vec{R}) \phi_{\text{el}}, \quad (7)$$

the latter being a solution to the nuclear Schrödinger equation in the effective potential generated by electrons

$$\left[- \frac{1}{R^2} \frac{\partial}{\partial R} \frac{R^2}{2 m_{\text{n}}} \frac{\partial}{\partial R} + \frac{J(J+1)}{2 m_{\text{n}} R^2} + \mathcal{E}_{\text{el}}(R) + \mathcal{E}_{\text{a}}(R) \right] \chi_{vJ}(R) = E_{\text{a}} \chi_{vJ}(R), \quad (8)$$

where the adiabatic correction to the BO potential $\mathcal{E}_{\text{el}}(R)$ is $\mathcal{E}_{\text{a}}(R) = \langle \phi_{\text{el}} | H_{\text{n}} | \phi_{\text{el}} \rangle_{\text{el}}$.

III. ROTATIONAL MAGNETIC MOMENT

The rotational magnetic moment of a molecule in a state with the rotational quantum number J is

$$\vec{\mu} = g \mu_{\text{N}} \vec{J}, \quad (9)$$

where g is the rotational g -factor and $\mu_N = e\hbar/(2m_p)$ is the nuclear magneton. In the leading order of the nonadiabatic perturbation theory, as in the adiabatic approximation, the g -factor is a function of the internuclear distance R . If we locate the origin of the molecule-fixed axis system in the geometrical center of the two nuclei, we can express the rotational g -factor of a diatomic molecule with equal nuclear charges as (see Eq. (98) of [2])

$$g(R) = \frac{m_p}{2m_n} \left(1 + \frac{2}{R^2} \left\langle \phi_{\text{el}} \left| \vec{J}_{\text{el}} \frac{1}{(\mathcal{E}_{\text{el}} - H_{\text{el}})'} \vec{J}_{\text{el}} \right| \phi_{\text{el}} \right\rangle_{\text{el}} \right), \quad (10)$$

where the integration goes over the electronic coordinates and where \vec{J}_{el} is the electronic component of the total angular momentum \vec{J} . The second term in parenthesis equals to $4m_n^2 \mathcal{W}_{\perp}(R)$ using the previously defined and evaluated function \mathcal{W}_{\perp} [10, 11]. On the other hand it is also equal to $4\chi_{\perp}^p(R)/R^2$ in terms of the paramagnetic susceptibility function [3, 4, 6].

To obtain the rotational magnetic moment for a given rovibrational level (v, J) we evaluate the expectation value (in units of μ_N)

$$\mu(v, J) = \langle \chi_{vJ} | g(R) | \chi_{vJ} \rangle J \quad (11)$$

with the nuclear wave functions χ_{vJ} , which are solutions to the radial nuclear equation (8). To obtain magnetic dipole transition rates we evaluate the off-diagonal matrix elements

$$T_J(v'' \rightarrow v') = \langle \chi_{v'J} | g(R) | \chi_{v''J} \rangle \mu_N, \quad (12)$$

between the states of the same, nonvanishing angular momentum (otherwise the matrix element of the magnetic dipole operator in Eq. (9) vanishes), whereas the probability of the M1 transition is given (in units of s^{-1}) by

$$A_J^{\text{M1}}(v'' \rightarrow v') = \frac{4}{3} (4\pi R_{\infty} c) \alpha^5 J(J+1) \times [\Delta E_J(v'' \rightarrow v')]^3 |T_J(v'' \rightarrow v')|^2, \quad (13)$$

where $\Delta E_J(v'' \rightarrow v')$ is the energy difference (in atomic units) between the higher (v'', J) and the lower (v', J) rovibrational level, $\alpha = 1/137.035999679(94)$ is the fine structure constant and $R_{\infty} c = 3.289841960361(22) \times 10^{15}$ Hz [12].

IV. RESULTS AND DISCUSSION

A. Magnetic moment

Details of evaluation of the $\mathcal{W}_{\perp}(R)$ function, which is directly related to $g(R)$ of Eq. (10), have been given in Refs. [10, 11] and will not be repeated here. The numerical values of the $g(R)$

function computed for H_2 are listed in Table I. To obtain analogous results for other isotopomers it is sufficient to rescale the data by pertinent nuclear reduced mass ratio, e.g. $m_n(\text{H}_2)/m_n(\text{D}_2)$ for D_2 or $m_n(\text{H}_2)/m_n(\text{HD})$ for HD . For $R \rightarrow \infty$, the second term in Eq. (10) goes to -1 and $g(\infty)$ vanishes regardless of the nuclear masses. At the $R = 0$ limit, the expression in parentheses equals to 1 so that $g(0) = m_p/(2m_n)$ and, via m_n , changes from one isotopomer to another. In evaluation of the nuclear reduced masses we used $m_p = 1836.15267247 m_e$ and $3670.4829654 m_e$ as the deuteron mass [12].

The rotational magnetic moment of H_2 , HD , and D_2 in their lowest rovibrational states has been determined experimentally by Ramsey and coworkers [5–9]. Several older and less precise experiments have also been reported [5, 6] but were omitted in the discussion here. For comparison with the outcome of the present work, shown in Table II, only the most accurate measurements were selected. The relative accuracy of the measurements is an order of magnitude higher than those of the computations. We estimate the relative accuracy of our theoretical results as equal to m_e/m_n . This error results from dropping higher order nonadiabatic terms. We also estimate that the omitted relativistic corrections to μ are even an order of magnitude smaller. Within this error estimation we note a very good agreement with the measurements.

Calculations of the rotational magnetic moment of the hydrogen molecule have already been performed by Rychlewski and Raynes [13], who employed Kołos-Wolniewicz wave functions to evaluate the magnetic susceptibility to a high accuracy. Using the connection between the perpendicular component of the paramagnetic susceptibility χ_\perp^p and the electronic part of the g -factor they evaluated the rotational g -factor for several rovibrational levels. The difference between their results and ours appears at most on the fourth significant figure. One should also mention some older calculations of the rotational magnetic moment, which were performed merely at the equilibrium internuclear distance and yielded an accuracy of about 10% [14]. Several other earlier attempts have also been reported in [15].

B. Magnetic dipole transitions

To our knowledge, the rotational magnetic dipole transitions in H_2 have not been studied yet. The main purpose of this paper is to report on the theoretical predictions of the transition intensities expressed through their probabilities $A_J^{\text{M}1}$ of Eq. (13). The accuracy of the $g(R)$ function, employed to evaluate the transition moment (12), has been verified in the previous section against experimental and other theoretical data. We further assume that the uncertainties assigned to μ

can be transferred directly to T_J . The energy separations ΔE_J were taken from our previous computations on H_2 [11, 16] and take into account all the adiabatic ($\sim m_n^{-1}$), nonadiabatic ($\sim m_n^{-2}$), relativistic ($\sim \alpha^2$) and radiative ($\sim \alpha^3$ and α^4) effects. Also the radial nuclear functions χ_{vJ} were obtained by solving the nonadiabatic version of Eq. (8) [11]. High accuracy of ΔE_J obtained with this procedure have been proven in confrontation with the measured values. For instance, the theoretically predicted lowest ortho–para separation in the $v = 0$ state of H_2 amounts to $118.486\,80(11)\text{ cm}^{-1}$ [16], which agrees up to $0.000\,04\text{ cm}^{-1}$ with the experiment [17]. We therefore assume that T_J is the only source of uncertainty in A_J^{M1} . Table III collects the M1 transition rates predicted for 30 rotational states of $v = 1 \rightarrow 0$ band of H_2 and D_2 .

The infrared spectrum of the H_2 molecule is dominated by the electric quadrupole (E2) transitions [18] (the electric dipole transitions are strongly forbidden). It is interesting to see if the magnetic dipole transitions could be competitive with respect to their intensity to E2 transitions. For this purpose we evaluated the probability A_J^{E2} of the E2 transition between the same rovibrational levels as for the M1 transition. The probability is given by the following formula

$$A_J^{\text{E2}}(v'' \rightarrow v') = \frac{1}{15} (4\pi R_\infty c) \alpha^5 \frac{J(J+1)}{(2J-1)(2J+3)} \times [\Delta E_J(v'' \rightarrow v')]^5 |T_J^{\text{E2}}(v'' \rightarrow v')|^2 \quad (14)$$

with $T_J^{\text{E2}}(v'' \rightarrow v') = \langle \chi_{v'J} | Q(R) | \chi_{v''J} \rangle$ and the quadrupole moment operator in the form $Q(R) = R^2/2 - \frac{1}{2} \langle \phi_{\text{el}} | \sum_a r_a^2 (3 \cos^2 \theta_a - 1) | \phi_{\text{el}} \rangle_{\text{el}}$. Our numerical results for A_J^{E2} agree with that of [19] to at least two significant digits.

The $v = 1 \rightarrow 0$ band transition probabilities of both types are compared in Figure 1. For the lowest J , the magnetic dipole transitions are almost three orders of magnitude weaker than the electric quadrupole transitions. For example, $A_1^{\text{M1}} = 7.13 \times 10^{-10}\text{ s}^{-1}$ whereas $A_1^{\text{E2}} = 4.28 \times 10^{-7}\text{ s}^{-1}$. With growing J though, the proportions change in favor of the M1 transition and for the highest rotational states the M1 intensities dominate unequivocally. Similarly, any magnetic dipole transitions with $\Delta J = 0$ are allowed and grow quickly with J . For convenience, we present in Table I values of $g(R)$, from which any magnetic dipole transition can be obtained if only the nuclear wave function of the initial and final state are known. An analogous M1 to E2 relation has been found for HD and D_2 . However HD exhibits much stronger electric dipole E1 transitions, which appear at different wavelength, as they corresponds to transitions with $\Delta J = 1$. Due to the smallness of the M1 transitions for low J , they probably have no astrophysical significance, however their existence should be most easily confirmed experimentally for the large values of J ,

by verifying the total transition rate as a sum of the E2 and M1 transitions.

Acknowledgments

KP acknowledges the support of NIST through the Precision Measurement Grant PMG 60NANB7D6153. JK acknowledges the support of the Polish Ministry of Science and Higher Education via Grant No. N N204 015338. Part of the computations has been performed within a computing grant from Poznań Supercomputing and Networking Center.

-
- [1] G. C. Wick, *Phys. Rev.* **73**, 51 (1948).
 - [2] K. Pachucki, *Phys. Rev. A* **81**, 032505 (2010).
 - [3] G. C. Wick, *Il Nuovo Cimento* (1924-1942) **10**, 118 (1933).
 - [4] G. C. Wick, *Z. Physik* **85**, 25 (1933).
 - [5] N. F. Ramsey, *Phys. Rev.* **58**, 226 (1940).
 - [6] N. J. Harrick and N. F. Ramsey, *Phys. Rev.* **88**, 228 (1952).
 - [7] R. G. Barnes, P. J. Bray, and N. F. Ramsey, *Phys. Rev.* **94**, 893 (1954).
 - [8] N. F. Ramsey, *Molecular Beams* (Oxford University Press, London, 1956).
 - [9] W. E. Quinn, J. M. Baker, J. T. LaTourrette, and N. F. Ramsey, *Phys. Rev.* **112**, 1929 (1958).
 - [10] K. Pachucki and J. Komasa, *J. Chem. Phys.* **129**, 034102 (2008).
 - [11] K. Pachucki and J. Komasa, *J. Chem. Phys.* **130**, 164113 (2009).
 - [12] 2006 CODATA recommended values, URL <http://www.physics.nist.gov/cuu/Constants>.
 - [13] J. Rychlewski and W. Raynes, *Mol. Phys.* **41**, 843 (1980).
 - [14] H.-W. Kim and H. F. Hameka, *Chem. Phys. Lett.* **32**, 241 (1975).
 - [15] H. F. Hameka, *Rev. Mod. Phys.* **34**, 87 (1962).
 - [16] K. Piszczatowski, G. Lach, M. Przybytek, J. Komasa, K. Pachucki, and B. Jeziorski, *J. Chem. Theory Comput.* **5**, 3039 (2009).
 - [17] D. E. Jennings, S. L. Bragg, and J. W. Brault, *Astrophys. J.* **282**, L85 (1984).
 - [18] J. M. Black and A. Dalgarno, *Astrophys. J.* **203**, 132 (1976).
 - [19] L. Wolniewicz, I. Simbotin, and A. Dalgarno, *Astrophys. J. Supp. Ser.* **115**, 293 (1998).

TABLE I: Internuclear distance dependence of the rotational magnetic g -factor for H_2 .

R/bohr	$g(R)$	R/bohr	$g(R)$
0.0	1.000 000	2.6	0.639 229
0.1	0.999 161	2.7	0.610 173
0.2	0.996 767	2.8	0.580 075
0.3	0.993 040	2.9	0.549 081
0.4	0.988 172	3.0	0.517 382
0.5	0.982 303	3.1	0.485 195
0.6	0.975 527	3.2	0.452 771
0.7	0.967 899	3.3	0.420 380
0.8	0.959 450	3.4	0.388 305
0.9	0.950 189	3.5	0.356 830
1.0	0.940 113	3.6	0.326 225
1.1	0.929 205	3.8	0.268 601
1.2	0.917 439	4.0	0.217 016
1.3	0.904 782	4.2	0.172 373
1.4	0.891 193	4.4	0.134 893
1.5	0.876 629	4.6	0.104 241
1.6	0.861 038	4.8	0.079 716
1.7	0.844 375	5.0	0.060 442
1.8	0.826 584	5.5	0.029 443
1.9	0.807 616	6.0	0.013 984
2.0	0.787 426	7.0	0.003 047
2.1	0.765 969	8.0	0.000 663
2.2	0.743 220	9.0	0.000 152
2.3	0.719 158	10.0	0.000 040
2.4	0.693 787	11.0	0.000 013
2.5	0.667 127	12.0	0.000 005

TABLE II: Comparison of the computed and measured rotational magnetic moments μ (in units of μ_N) for the hydrogen molecule in the lowest vibrational state ($v = 0$).

J	H ₂	HD	D ₂
1 Theory	0.8825(10)	0.6629(5)	0.4428(2)
Experiment	0.882910(80) [8]	0.663211(14) [9]	0.442884(52) [7]
2 Theory	1.764(2)	1.325(1)	0.8853(5)
Experiment	1.764530(70) [7]		

TABLE III: Rates of the M1 (A_J^{M1}) and E2 (A_J^{E2}) transitions, in units of $10^{-8} s^{-1}$, for the rotational states of $v = 1 \rightarrow 0$ band in H_2 and D_2 . The relative uncertainty of A_J^{M1} and A_J^{E2} is $2 m_e/m_n$ and comes from the neglected higher order nonadiabatic effects.

J	H_2		D_2	
	A_J^{M1}	A_J^{E2}	A_J^{M1}	A_J^{E2}
1	0.07131	42.84	0.004508	5.850
2	0.2140	30.27	0.013527	4.157
3	0.4282	27.79	0.02706	3.849
4	0.7140	26.48	0.04512	3.710
5	1.072	25.43	0.06770	3.614
6	1.501	24.41	0.09482	3.531
7	2.002	23.37	0.1265	3.450
8	2.575	22.27	0.1627	3.366
9	3.218	21.11	0.2034	3.279
10	3.932	19.89	0.2487	3.186
11	4.715	18.63	0.2986	3.088
12	5.566	17.34	0.3529	2.986
13	6.482	16.03	0.4118	2.878
14	7.461	14.71	0.4751	2.767
15	8.500	13.40	0.5429	2.652
16	9.594	12.10	0.6150	2.533
17	10.74	10.84	0.6914	2.413
18	11.93	9.615	0.7720	2.290
19	13.16	8.446	0.8568	2.166
20	14.41	7.337	0.9455	2.042
21	15.69	6.296	1.038	1.9180
22	16.96	5.330	1.135	1.7946
23	18.23	4.443	1.234	1.6726
24	19.46	3.639	1.338	1.5525
25	20.64	2.920	1.444	1.4348
26	21.73	2.287	1.553	1.3200
27	22.69	1.740	1.665	1.2086
28	23.48	1.277	1.779	1.1009
29	24.04	0.8953	1.894	0.9974
30	24.29	0.5914	2.011	0.8984

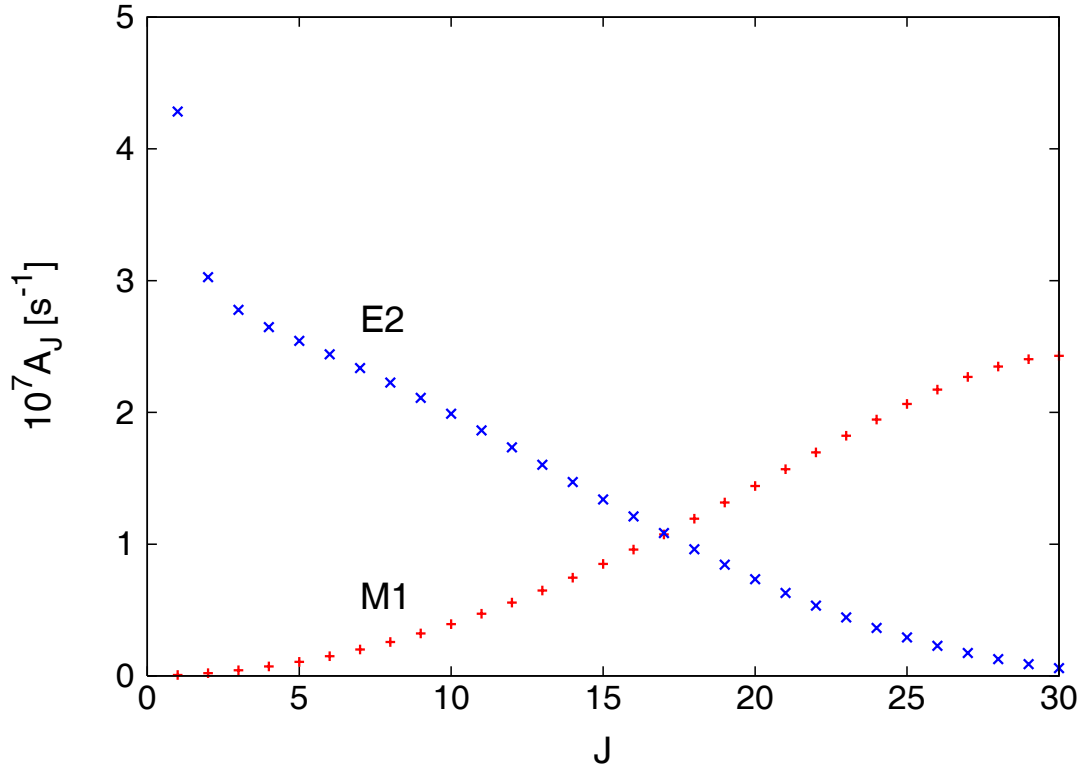


FIG. 1: (Color online) Comparison of the rates of the magnetic dipole transition (M1) with the $\Delta J = 0$ electric quadrupole transition (E2) in H_2 .